International Journal of Advanced Trends in Engineering and Technology (IJATET)
Impact Factor: 5.665, ISSN (Online): 2456 - 4664
(www.dvpublication.com) Volume 2, Issue 2, 2017

GROWTH AND STUDIES OF AMMONIUM CADMIUM SULFATE HYDRATE CRYSTALS

M. Andiappan*, P. Selvarajan & S. Perumal***
* Physics Research Centre, S.T Hindu College, Nagercoil, Tamilnadu
** Department of Physics, Aditanar College of Arts and Science, Tiruchendur, Tamilnadu

Cite This Article: M. Andiappan, P. Selvarajan & S. Perumal, "Growth and Studies of Ammonium Cadmium Sulfate Hydrate Crystals", International Journal of Advanced Trends in Engineering and Technology, Volume 2, Issue 2, Page Number 29-34, 2017.

Abstract:

Ammonium cadmium sulfate hydrate (ACSH) crystals were grown by solution method at room temperature. Single crystals of ACSH were subjected to XRD studies to reveal the crystal structure. The functional groups of the sample have been identified by FTIR studies. Linear optical constants were determined by UV-visible spectral studies. Mechanical properties have been evaluated by Vickers hardness method. Dielectric studies for the sample were carried out using a two-probe arrangement and an LCR meter at different temperatures and frequencies. The thermal stability of the sample was checked by TG/DTA studies and the results are discussed in this paper.

1. Introduction:

Tutton salts are formed by combining a monovalent cation such as potassium, rubidium, cesium or ammonium and a divalent cation such as magnesium, vanadium, chromium, manganese, iron, cobalt, nickel, copper, zinc or cadmium [1-3]. Usually they crystallize in a monoclinic system and these salts have various applications linked especially to the optical properties of the transition metals. They are used in the developments concerning domestic heating and hot-water supply because of their high melting temperatures and high enthalpies of fusion, as well in fertilizer industry as ionic conductors [4-7]. These salts are named after E.H.Tutton, who synthesized and characterized a large number of salts and they are used as reliable reagents and spectroscopic standards [8, 9]. It is observed that various studies of a large number of Tutton salts have been reported in the literature [10-14]. Since detailed studies on growth and characterization of ammonium cadmium sulfate have not been reported in the literature, the concentration has been paid here on various studies of ammonium cadmium sulfate (ACSH) crystals.

2. Synthesis and Growth of Ammonium Cadmium Sulfate Crystals:

Ammonium sulfate and cadmium sulfate were used as the starting materials for the synthesis of ammonium cadmium sulfate hydrate (ACSH) salt and the reactants were taken in 1:1 molar ratio, were dissolved in double distilled water. The saturated solution was kept in a hot water bath at 50^{o}C to obtain the synthesized salt of ACSH. The seed crystals were prepared by spontaneous nucleation. The crystals were grown by slow and controlled evaporation using the synthesized salt of ACSH in a constant temperature bath. Single crystals of ACSH have been grown over a period of 1 month and the harvested crystal of ACSH is shown in the figure 1. It is observed that the grown crystal is transparent, non-hygroscopic and colourless.

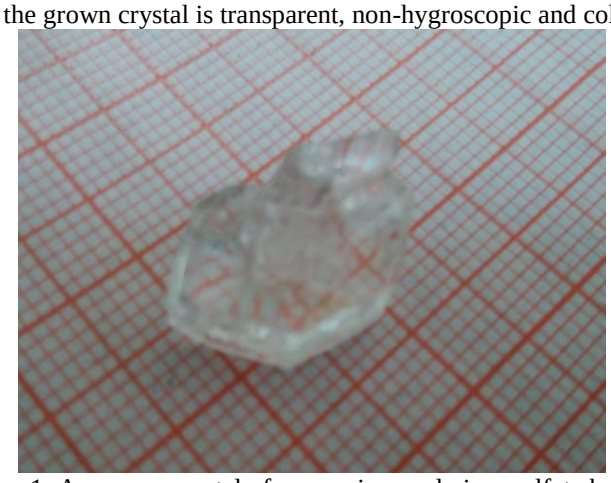

Figure 1: As-grown crystal of ammonium cadmium sulfate hydrate

3. XRD Studies:

Single crystal X-ray diffraction analysis was carried out to determine the lattice parameters of ammonium fluoro antimonate crystal. The lattice parameters and hence the structure were obtained for the sample using a ENRAF NONIUS CAD4 X-ray diffractometer with MoK_{α} radiation (λ = 0.71069 Å). The obtained lattice parameters for the sample are a = 9.427(6) Å, b = 12.836(4) Å, c = 6.302(2) Å, $\alpha = 90^{\circ}$, $\beta = 105.52^{\circ}$, $\gamma = 90^{\circ}$. It is observed that ACSH crystal belongs to monoclinic system with the number molecular units per unit cell Z=2. The volume of monoclinic unit cell is found from the relation V =a b c sin β and the

obtained value is 736.31 (3) $Å^3$. The space group of the system is $P2_1/a$ and it is recognized as centrosymmetric space group. The molecular weight of ACSH crystal is 448.69 and the density of the crystal was found to be 2.022 g/cc.

4. FTIR Analysis:

IR spectra originate in transitions between two vibrational levels of a molecule in the electronic ground state and are usually observed as absorption spectra in the infrared region. For a molecule to present infrared absorption bands it is needed that it has a permanent dipole moment. When a molecule with at least one permanent dipole vibrates, this permanent dipole also vibrates and can interact with the oscillating electric field of incident infrared radiation. In order for this normal mode of vibration of the molecule to be infrared active, that is, to give rise to an observable infrared band, there must be a change in the dipole moment of the molecule during the course of the vibration [15, 16]. The FTIR spectrum of the sample were recorded using a Perkin-Elmer FTIR spectrometer using KBr pellet technique in the range 4000-400 cm^{-1} and it is presented in the fig.2. The peaks observed at 3325 cm^{-1} and 3130-cm^{-1} are due to the presence of OH asymmetric and symmetric stretching vibrations. Bending vibrations of water molecules are observed at 1617 cm^{-1}. S = O stretching vibration is noticed at 1402 cm^{-1}. SO_4^{2-} stretching and degenerate vibrations are observed at 1119 and 615 cm^{-1}. The FTIR assignments for ACSH crystal are provided in the table 1.

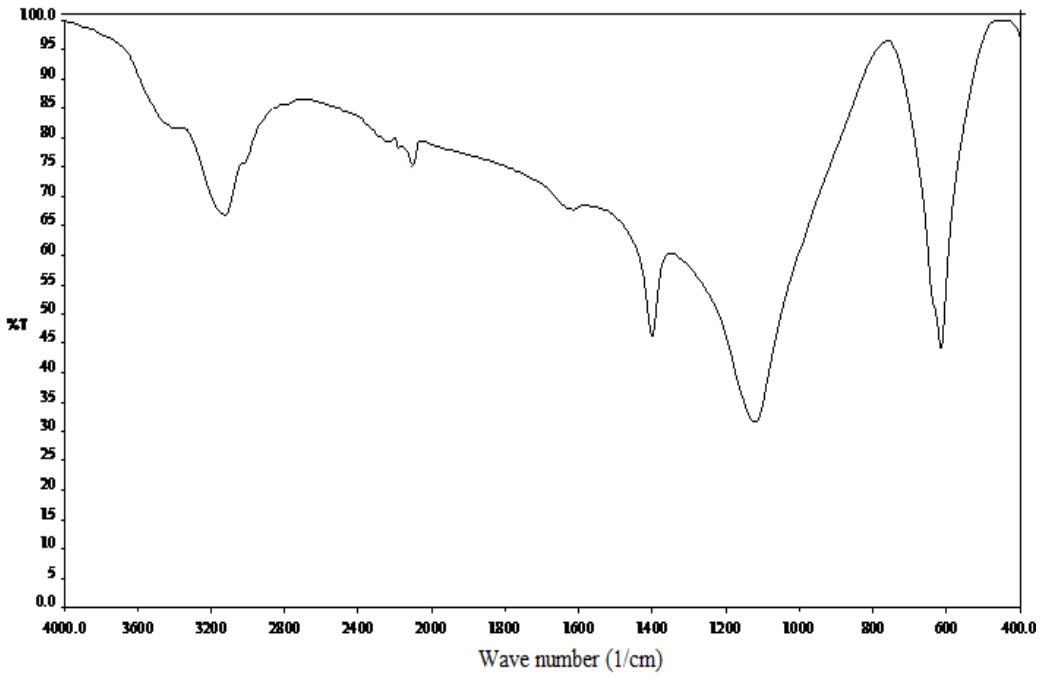

Figure 2: FTIR spectrum of ammonium cadmium hydrate sulfate crystal

Wave number (cm^{-1})	Assignments
	OH asymmetric stretching
3325	OH symmetric stretching
3130	Bending vibrations of water
1617	molecules
1402	S= O stretching
1119	SO_4^{2-} stretching
615	Degenerate vibrations of SO_4^{2-}

Table 1: FTIR assignments for ACSH crystal

5. UV- Visible Spectral Studies:

The UV-visible spectrophotometer uses two light sources, a deuterium (D2) lamp for ultraviolet light and a tungsten (W) lamp for visible light. After bouncing off a mirror, the light beam passes through a slit and hits a diffraction grating. The grating can be rotated allowing for a specific wavelength to be selected. At any specific orientation of the grating, only monochromatic successfully passes through a slit. A filter is used to remove unwanted higher orders of diffraction. The light beam hits a second mirror before it gets split by a half mirror. One of the beams is allowed to pass through a reference cuvette, the other passes through the sample cuvette. The intensities of the light beams are then measured at the end. Molecules containing π-electrons can absorb the energy in the form of ultraviolet or visible light to excite these electrons to higher molecular orbitals.

The ultraviolet-visible-near infrared transmittance spectral studies were carried out using a Perkin-Elmer Lambda 35 spectrophotometer in the wavelength range 200-1100 nm. The recorded spectrum of ACSH crystal is shown in figure 3. From the results, it is noticed that there is less absorption of light in the visible range of electromagnetic spectra and this is the intrinsic property of sample and this clearly indicates that it can be used as window materials in optical instruments. For optical fabrications, a crystal should be highly transparent in a considerable region of wavelength. The obtained cut-off wavelength for the sample is 210 nm. The optical band gap for ACSH crystal was determined using the relation $E_g = 1242 / \lambda$ and the obtained value for the sample is 5.914 eV. Hence, the sample is a wide band gap material.

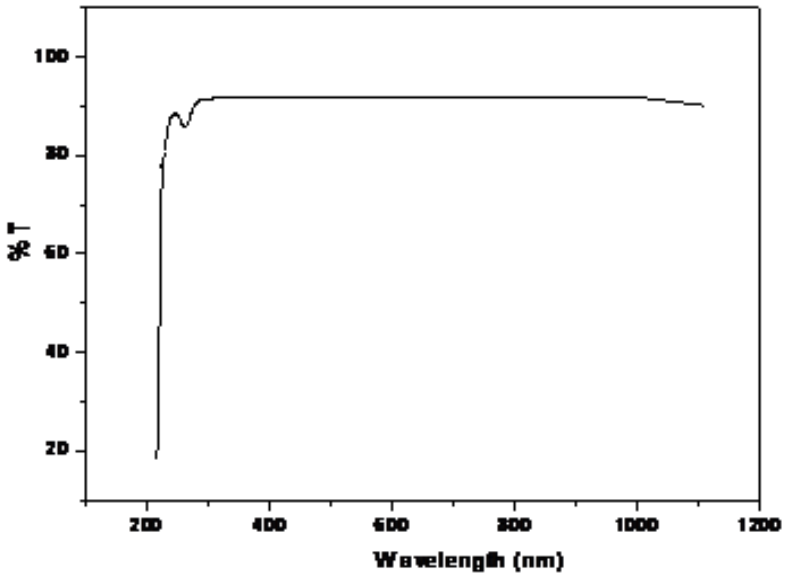

Figure 3: UV-visible spectrum of ACSH crystal

6. TG/DTA Thermal Analysis:

Thermogravimetric (TG) analysis is a type of thermo analytical testing performed on materials to determine changes in weight in relation to changes in temperature. TG relies on a high degree of precision in three measurements viz. weight, temperature, and temperature change. TG is commonly employed in research and testing to determine characteristics of materials, to determine degradation temperatures, absorbed moisture content of materials, the level of inorganic and organic components in materials, decomposition points of explosives, and solvent residues. In differential thermal analysis (DTA), the heat absorbed or emitted by a chemical system is observed by measuring the temperature difference between the system and an inert reference compound such as alumina, silicon carbide or glass beads.

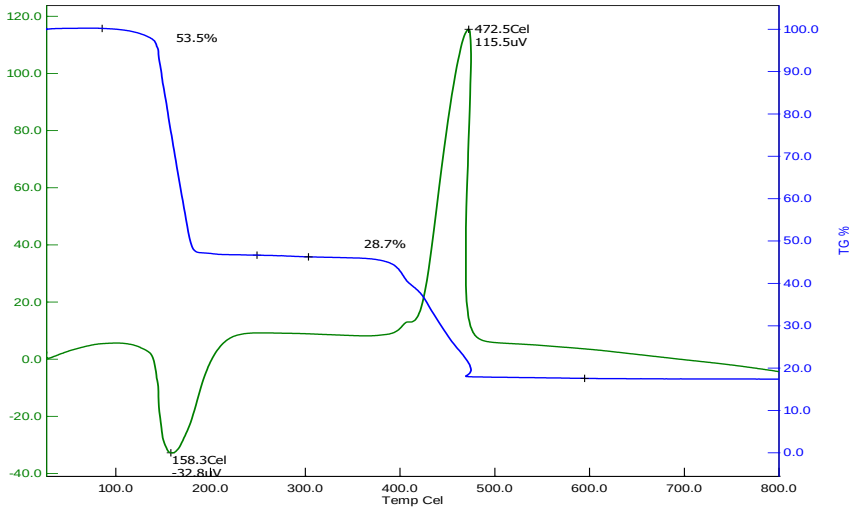

Figure 4: TG/DTA thermal curves for ACSH crystal

As the temperature of both is increased at a constant rate, the corresponding deviation of the sample temperature from that of the reference temperature versus the programmed temperature is recorded and it explains whether the transition is endothermic or exothermic. DTA and TG analyses are often run

simultaneously on a single sample and the TG/DTA studies were carried out using a SDT Q600 V8.3 Build 101 thermal analyzer in the temperature range from ambient temperature to 800 ºC at the heating rate of 20 ºC/min in nitrogen atmosphere. The recorded TG/DTA thermal curves for ACSH crystal is presented in the figure 4. The TG/DTA studies establish that the sample is thermally stable upto its melting points/decomposition points. From the results, it is observed that the sample loses water molecules below 160 ^{o}C and hence it is thermally stable upto 160 ^{o}C. About 54% of weight of the sample is reduced due to removal of water molecules from the sample. Here this temperature can be considered as the decomposition point of the sample. The exothermic peak at 472.5 ^{o}C is corresponding to release of gaseous particles from the sample. It is noticed that there is no residues of the sample left in the temperature range 500-800 C.

7. Microhardness Studies:

Hardness is one of the important mechanical properties of solid material. It can be used as a suitable measure of the plastic properties and strength of the material. Transparent crystals free from cracks were selected for microhardness measurements. Before indentations, the crystal was carefully lapped and washed to avoid surface effects. Microhardness analyses were carried out using Shimadzu Vickers microhardness tester fitted with a diamond indenter attached to an incident light microscope. The well polished ACSH crystal was placed on the platform of the Vickers microhardness tester and the loads of different magnitude were applied over a fixed interval of time. The indentation time was kept as 10 sec for all the loads and the microhardness number was determined using the relation $H_v = 1.8544\ P/d^2$. The variation of hardness number with the applied load for the sample is shown in the figure 5. The results show that hardness number increases gradually upto 75 grams and then it decreases and this indicates that the sample could withstand the weight upto 75 grams. The increasing part of the curve is due to the reverse indentation size effect and the decreasing part of the curve is due the direct indentation size effect [17, 18]. It is observed that there are cracks formed in the sample when a weight more than 75 g was applied to the sample.

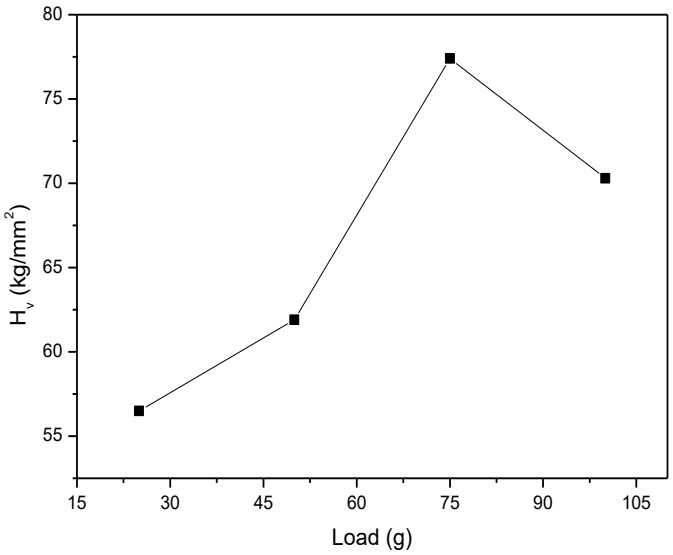

Figure 5: Variation of hardness number with applied load for ACSH crystal

8. Dielectric Properties:

A dielectric is an electrical insulator that can be polarized by applied electric field. When a dielectric is placed in an electric field, the electric charges do not flow through the material as they do in conductor, but slightly shift from their average equilibrium positions causing dielectric polarization. Because of dielectric polarization, positive charges are displaced towards the field and negative charges shift in the opposite direction. This creates an internal electric field which reduces the overall field within the dielectric itself. If a dielectric is composed of weakly bonded molecules, those molecules not only become polarized, but also reorient so that their symmetry axis aligns to the field. A capacitor filled with a dielectric material has a real capacitance ε_r times greater than a capacitor with the same electrodes in vacuum. The relative permittivity of a material under given conditions reflects the extent to which it concentrates electrostatic line of flux. In technical terms, it is the ratio of the amount of electrical energy stored in a material by an applied voltage, relative to that stored in a vacuum. It is also the ratio of the capacitance of capacitor using that material as a dielectric, compared to a similar capacitor that has a vacuum as its dielectric. The dielectric constant of any given material varies with temperature and also varies as a function of frequency. When a dielectric is placed in an alternating field, the four types of polarizations set up in the material and the dielectric constant is a consequence of them. There will

be a temporal phase shift found to occur between the driving field and the resulting polarization thereby loss current component appears. It gives the dielectric loss of the sample. The amount of power losses in a dielectric material under the action of the voltage applied to it is commonly known as dielectric losses which usually mean the losses precisely under an alternating voltage. The dielectric loss angle is an important parameter both for the dielectric material and an insulated portion [19, 20]. The capacitance and dielectric loss factor (tan δ) measurements were carried out using the parallel plate capacitor at various temperatures ranging from 30° - 70°C using an Agilent 4284A LCR meter at different frequencies ranging from 100 Hz to 1MHz. Contact faces of the crystal are coated by graphite to obtain a good conductive surface layer. The dielectric constant (ε_r) is calculated using the relation $\varepsilon_r = (C\ d)/(\varepsilon_0\ A)$ where C is the capacitance, d is the thickness of the sample, A is the area of the electrode contact and ε_0 is the permittivity of the free space. The accuracy involved in the measurements of dielectric parameters was within ±5% and the temperature of the sample was measured using a thermocouple. Figures 6 and 7 show the variations of dielectric constant and loss factor with temperature at different frequencies of 1000 Hz, 10 kHz, 1000 kHz. It is seen from the plots that the dielectric constant is relatively high in the lower frequency region and then decreases with applied frequency. The high values of dielectric constant at low frequencies may be due to the presence of combinations of polarizations namely space charge and orientational polarizations. Increase of dielectric constant and loss factor with temperature may be due to the thermal excitation of atoms about their lattice points, expansion of crystal and blocking of charge carriers at the electrodes. There is no ferroelectric transition in the temperature range 30-80 ^oC because ACSH crystal has the ferroelectric transition at 87 K.

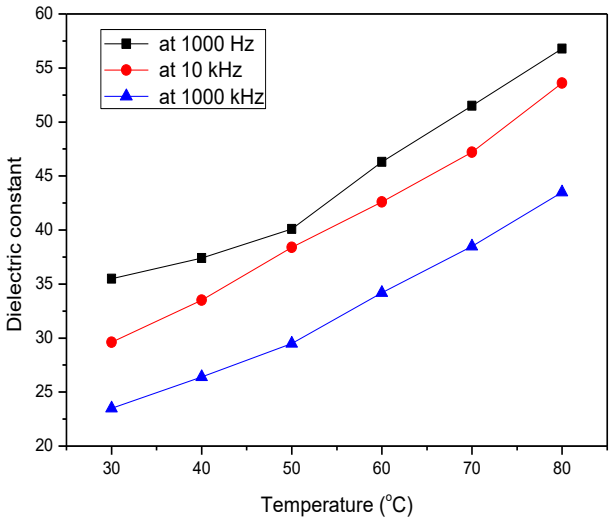

Figure 6: Variation of dielectric constant with temperature at different frequencies for ACSH crystal

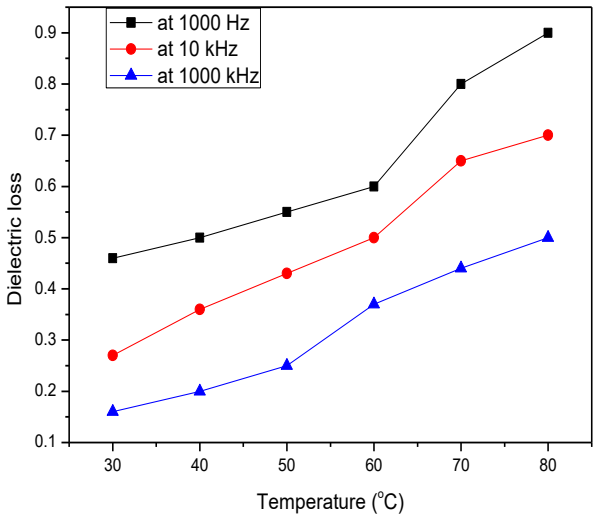

Figure 7: Variation of dielectric loss with temperature at different frequencies for ACSH crystal

9. SHG Studies:

Second harmonic generation (SHG) is also called as frequency doubling and the SHG efficiency was measured by Kurtz powder technique [21]. A Nd:YAG laser operating at 1064 nm was used as the source and the laser light was directed on the sample and the emitted light is collected, filtered and detected with a photomultiplier tube. The generation of second harmonics was not confirmed as the grown crystal is not found to produce green light. Hence, ACSH sample is a centrosymmetric crystal at room temperature. Below the ferroelectric transition temperature (87 K), the sample is changed to a ferroelectric material and it may show second harmonics below 87 K.

10. Conclusion:

Good quality optical single crystals of ammonium cadmium sulfate hydrate (ACSH) were grown using slow evaporation technique. The lattice parameters of grown crystal have been identified from XRD studies. The absorption frequencies of the sample have been found by FTIR spectral studies. The UV-visible spectral study reveals that the material has a wide optical transparency window in the entire visible region with a cutoff at 210 nm. The thermal stability of the sample was checked by TG/DTA studies. XRD and SHG studies reveal that ACSH crystal is a centrosymmetric and hence it does not emit visible laser light under IR laser irradiation. Ferroelectric transition was not observed for ACSH crystal in the temperature range 30-80 ^{o}C.

11. Acknowledgement:

Authors have gratefully acknowledged the management committee members of the Aditanar College of Arts and Science, Tiruchendur and S.T Hindu College, Nagercoil for the constant encouragement given to them to carry out the research work.

12. References:

1. V. Ananthanaeayanan, Z. Phys. 163 (1961) 144.
2. W. Y. Kim, A. R. Lim, J. Therm. Anal. Calorim. 116 (2014) 779.
3. P.S. Rao, Spectrochim. Acta A 52 (1996) 1127.
4. H. Anandalakshmi, S. Parthiban, V. Parvathi, V. Thanikachalam, S.C. Mojumdar, J. Therm. Anal. Calorim. 104 (2011) 963.
5. G. Ramasamy, G. Bhagavannarayana, G. Madhurambal, Subbiah Meenakshisundaram, J. Cryst. Growth 352 (2012) 137.
6. A. Ran Lim, J. Ha Lee, Phys. Status Solidi B 247 (2010) 1242.
7. P.S. Rao, Spectrochim. Acta A 52 (1996) 1127.
8. P. Chand, R. Murali Krishna, J. Lakshmana Rao, S.V.J. Lakshman, Radiat. Eff. Defects Solids 127 (1993) 245.
9. W. Voigt, S. Goring, Thermochim. Acta 231 (1994) 13.
10. F. Bosi, G. Belardi, P. Ballirano, Am. Mineral. 94 (2009) 74.
11. H. Anandalakshmi, T.M. Rajendiran, R. Venkatesan, P. Sambasiva Rao, Spec- trochim. Acta A 56 (2000) 2617.
12. A.C. De Vroomen, E.E. Lijphart, N.J. Poulis, Physica 47 (1970) 458.
13. P. Sambasiva Rao, Spectrochim. Acta A 49 (1993) 897. [19] M. Georgiev, D. Marinova, D. Stoilova, Vib. Spectrosc. 53 (2010) 233.
14. Albert N. L., Keiser W.E. and Szymanski H. A., IR theory,Practice of IR Spectroscopy Plenum Press, New York (1973).
15. Nagamoto K., IR and Raman Spectra of Inorganic and coordination compounds, John Wiley and Sons New York (1978).
16. A. Szymanski, J.M. Szymanski, Hardness estimation of materials: rocks and ceramic material, PWN-Polish Scientific publishing, Warsaw (1989).
17. B.W. Mott, Micro Indentation Hardness Testing, Butterworths, London, 1956.
18. K. V. Rao, A. A. Smakula, J. Appl. Phys. 36 (1965) 2031.
19. P. Selvarajan, B. N. Das, H. B. Gon, K. V. Rao, J. Mater. Sci. 29 (1994) 4061.
20. S. K. Kurtz, T. T. Perry, J. Appl. Phys, 39, (1968) 3798.